

# Nitrogen cycling microbiomes are structured by plant mycorrhizal associations with consequences for nitrogen oxide fluxes in forests

Ryan M. Mushinski<sup>1,2</sup>  | Zachary C. Payne<sup>2,3</sup> | Jonathan D. Raff<sup>2,3</sup>  |  
Matthew E. Craig<sup>4,5</sup>  | Sally E. Pusede<sup>6</sup>  | Douglas B. Rusch<sup>7</sup>  | Jeffrey R. White<sup>2,8</sup>  |  
Richard P. Phillips<sup>4</sup> 

<sup>1</sup>School of Life Sciences, University of Warwick, Coventry, UK

<sup>2</sup>O'Neill School of Public and Environmental Affairs, Indiana University, Bloomington, IN, USA

<sup>3</sup>Department of Chemistry, Indiana University, Bloomington, IN, USA

<sup>4</sup>Department of Biology, Indiana University, Bloomington, IN, USA

<sup>5</sup>Environmental Sciences Division and Climate Change Science Institute, Oak Ridge National Laboratory, Oak Ridge, TN, USA

<sup>6</sup>Department of Environmental Sciences, University of Virginia, Charlottesville, VA, USA

<sup>7</sup>Center for Genomics and Bioinformatics, Indiana University, Bloomington, IN, USA

<sup>8</sup>Department of Earth and Atmospheric Sciences, Indiana University, Bloomington, IN, USA

## Correspondence

Ryan M. Mushinski, University of Warwick, Gibbet Hill Campus, Coventry CV4 7AL, UK.  
Email: Ryan.Mushinski@warwick.ac.uk

## Funding information

US Department of Agriculture, Grant/Award Number: 2013-67011-21095; US Department of Energy Joint Genome Institute, Grant/Award Number: DE-AC02-05CH11231; US Department of Energy, Grant/Award Number: DE-SC0014443; US Department of Agriculture National Institute of Food and Agriculture, Grant/Award Number: 2018-08037; NSF, Grant/Award Number: AGS-1352375; Oak Ridge National Laboratory, Grant/Award Number: DE-AC05-00OR22725

## Abstract

Volatile nitrogen oxides ( $\text{N}_2\text{O}$ ,  $\text{NO}$ ,  $\text{NO}_2$ ,  $\text{HONO}$ , ...) can negatively impact climate, air quality, and human health. Using soils collected from temperate forests across the eastern United States, we show microbial communities involved in nitrogen (N) cycling are structured, in large part, by the composition of overstory trees, leading to predictable N-cycling syndromes, with consequences for emissions of volatile nitrogen oxides to air. Trees associating with arbuscular mycorrhizal (AM) fungi promote soil microbial communities with higher N-cycle potential and activity, relative to microbial communities in soils dominated by trees associating with ectomycorrhizal (ECM) fungi. Metagenomic analysis and gene expression studies reveal a 5 and 3.5 times greater estimated N-cycle gene and transcript copy numbers, respectively, in AM relative to ECM soil. Furthermore, we observe a 60% linear decrease in volatile reactive nitrogen gas flux ( $\text{NO}_y \equiv \text{NO}$ ,  $\text{NO}_2$ ,  $\text{HONO}$ ) as ECM tree abundance increases. Compared to oxic conditions, gas flux potential of  $\text{N}_2\text{O}$  and  $\text{NO}$  increase significantly under anoxic conditions for AM soil (30- and 120-fold increase), but not ECM soil—likely owing to small concentrations of available substrate ( $\text{NO}_3^-$ ) in ECM soil. Linear mixed effects modeling shows that ECM tree abundance, microbial process rates, and geographic location are primarily responsible for variation in peak potential  $\text{NO}_y$  flux. Given that nearly all tree species associate with either AM or ECM fungi, our results indicate that the consequences of tree species shifts associated with global change may have predictable consequences for soil N cycling.

## KEYWORDS

forest soils, metagenomes, mycorrhizae, nitrogen cycle, nitrous oxide, reactive nitrogen oxides

This is an open access article under the terms of the Creative Commons Attribution License, which permits use, distribution and reproduction in any medium, provided the original work is properly cited.

© 2020 The Authors. *Global Change Biology* published by John Wiley & Sons Ltd

## 1 | INTRODUCTION

One of the major pathways for nitrogen (N) loss in forest soil is through volatilization of reduced N (e.g., nitrogen oxides). Studies in North America have illustrated that anthropogenic sources of nitrogen oxides to air have declined significantly over the past two decades, including an estimated 4% decrease since 2005 (Jiang et al., 2018; Romer et al., 2018; Simon et al., 2015). However, increases in the use of N-based fertilizers (Bouwman et al., 2002; Lu & Tian, 2017), warmer global temperatures (Hansen et al., 2010), and land-use change (Jain et al., 2013; Wang et al., 2017) have increased the importance of non-anthropogenic sources, such as soil, to the global N budget. Nitrous oxide ( $\text{N}_2\text{O}$ ) and the suite of volatile reactive nitrogen oxide compounds ( $\text{NO}_y \equiv \text{NO}, \text{NO}_2, \text{HONO}$ , etc.) are major products that have profound effects on climate and atmospheric chemistry.  $\text{N}_2\text{O}$  is one of the most potent greenhouse gases with roughly 300 times the global warming potential of carbon dioxide ( $\text{CO}_2$ ), and has been shown to deplete stratospheric ozone ( $\text{O}_3$ ) (Finlayson-Pitts & Pitts Jr., 2000). Additionally,  $\text{NO}_y$  species drive photochemical ozone production, are precursors to acid rain (via  $\text{HNO}_3$ ), and influence the oxidizing capacity of the atmosphere by sustaining photocatalytic cycles of  $\text{HO}_x$  (Bouwman et al., 2002; Steinkamp et al., 2009). While N emissions from agricultural systems are well characterized, significantly less is known about the sources and sinks of nitrogen oxides in natural ecosystems, such as upland forest soils, as well as the environmental properties and conditions that influence  $\text{N}_2\text{O}$  and  $\text{NO}_y$  flux.

Microbial oxidation and reduction drive the vast majority of soil nitrogen oxide fluxes. The biological cycling of  $\text{N}_2\text{O}$  and  $\text{NO}_y$  can be directly linked to various microbial processes, primarily nitrification and denitrification but also assimilatory and dissimilatory nitrate reduction (ANRA/DNRA; Figure 1). The rate-limiting step for nitrogen oxide production is generally considered to be associated with nitrification, which is defined as a cascade of oxidative metabolism from ammonia to nitrate. This process can be identified by the activities of ammonia-oxidizing archaea (AOA) and bacteria (AOB) as well as nitrite-oxidizing bacteria (NOB), which have all been linked to  $\text{N}_2\text{O}$  and  $\text{NO}_y$  production under oxic conditions (Mushinski et al., 2019; Robertson & Tiedje, 1987; Scharko et al., 2015). Specifically, nitrification-derived  $\text{NO}_y$  and  $\text{N}_2\text{O}$  have been correlated to the abundance of nitrification genes and transcripts (Soares et al., 2016). The most common targets include genes associated with ammonia monooxygenase (AMO), hydroxylamine oxidoreductase (HAO), and nitrite oxidoreductase (NXR). Although aerobic nitrifiers are considered rate limiting and can contribute to fluxes of  $\text{N}_2\text{O}$  and  $\text{NO}_y$ , most emissions are thought to be a function of denitrifying heterotrophic microbes, albeit through processes associated with reducing conditions such as assimilatory and dissimilatory nitrate reduction, as well as the multi-step reduction of nitrite to  $\text{N}_2$  (Ambus & Zechmeister-Boltenstern, 2007). Microbial groups associated with denitrification are highly diverse, but their relative abundance and activity can be determined by quantifying the abundance of gene and transcript copies associated with reduction of nitrate (NAR/NAP), nitrite

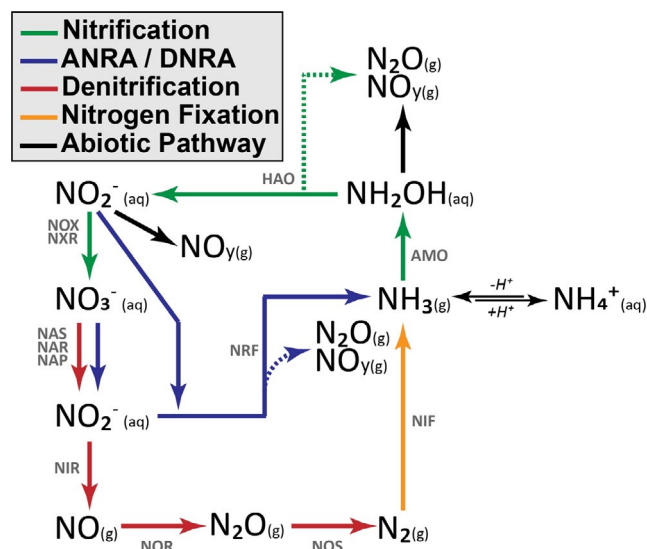


**FIGURE 1** Simplified diagram showing the enzymatic steps for nitrification, assimilatory and dissimilatory nitrate reduction to ammonia (ANRA/DNRA), denitrification, and nitrogen fixation processes. Dashed lines indicate production of gaseous byproducts of enzyme activity. Enzymes are noted above pathways. AMO: ammonia monooxygenase; HAO: hydroxylamine oxidoreductase; NOX/NXR: nitrate oxidoreductase; NAS/NAR/NAP: nitrate reductase; NRF/NIR: nitrite reductase; NOR: nitric oxide reductase; NOS: nitrous oxide reductase; NIF: nitrogenase reductase

(NIR), nitric oxide (NOR), and nitrous oxide (NOS) (Levy-Booth et al., 2014). Reducing conditions lead to upregulation of these denitrification genes, a situation commonly found in anoxic soil microsites, resulting in hotspots of  $\text{N}_2\text{O}$  and  $\text{NO}_y$  flux (Kuzakov & Blagodatskaya, 2015). Therefore, there is a need to quantify nitrogen oxide fluxes and the associated microbial responses to varying oxygen conditions.

Forest soil microbial communities are strongly influenced by vegetation composition (Lladó et al., 2017). Considering that forests are currently experiencing large-scale shifts in tree species composition (Jo et al., 2019), due to natural and anthropogenic effects such as climate change, atmospheric deposition, alterations in disturbance, habitat fragmentation, and exotic species invasion, there is a need to develop robust frameworks for investigating the microbial and biogeochemical consequences of such changes. Forests within the United States are comprised of a mixture of tree species that associate primarily with either arbuscular mycorrhizal fungi (AM) or ectomycorrhizal fungi (ECM). Examples of AM tree genera include maple (*Acer*), tulip (*Liriodendron*), cherry (*Prunus*), and ash (*Fraxinus*) while ECM tree genera include oak (*Quercus*), hickory (*Carya*), and beech (*Fagus*). Given that AM and ECM trees possess different nutrient use traits (Beidler et al., 2020; Cheeke et al., In press; Keller & Phillips, 2019; Lin et al., 2017) and promote unique soil microbial assemblages (Cheeke et al., 2017), the relative abundance of AM or ECM trees in a stand may be an effective integrator of various ecosystem processes (Phillips et al., 2013). Researchers have used the AM and ECM categorization to reflect distinct biogeochemical syndromes (e.g., AM: inorganic nutrient

economy, fast N cycling; ECM: organic nutrient economy, slow N cycling). Consequently, “mycorrhizal gradients” (defined as plots varying in their relative abundance of AM vs. ECM trees within an ecosystem) have been proposed as an appropriate experimental “proving ground” for exploring the effect of species shifts on biogeochemical processes in these forest ecosystems (Jo et al., 2019).

Numerous studies have observed that AM and ECM forests differ with respect to N cycling (Craig et al., 2018; Lin et al., 2017; Midgley & Phillips, 2014; Zhu et al., 2018). AM soils tend to possess low C:N ratios, large pools of inorganic N, and high rates of nitrification and are generally referred to as having “open” N cycles (e.g., high N loss relative to N recycled); conversely, ECM soils possess wide C:N ratios, large pools of organic N, and low rates of net nitrification and are referred to as having “closed” N cycles. Read (1991) first illustrated differences between AM and ECM soil N cycling, hypothesizing that ECM soils have lower nitrogen mineralization rates (relative to AM soils) owing to the large amounts of N bound to soil organic matter. More recently, Phillips et al. (2013) hypothesized that the abundance of AM and ECM trees in a plot, stand, or region may provide an integrated index of N cycling. The framework proposed by Phillips is supported by a recent meta-analysis (Lin et al., 2017), which used a global dataset to illustrate that inorganic N concentrations, net N mineralization, and nitrification rates are all higher in AM relative to ECM forests; however, we have a limited understanding of the underlying microbial contributions to the patterns, and the consequences for N retention and loss. Furthermore, the high rates of N-cycle activity in AM soil, under oxic conditions, may be exacerbated as soil becomes more anoxic. Thus, comparing N-gas fluxes and microbial activity under a factorial combination of oxic and anoxic conditions in AM and ECM soil will help better define these hotspots and hot moments in forest soils.

Recently, Mushinski et al. (2019) reported that AM soils produce significantly higher fluxes of  $\text{NO}_y$  under oxic conditions, relative to ECM soils at a single site. However, the following questions remain: To what extent do microbial communities involved in N cycling differ across mycorrhizal gradients within temperate forests, what are the influences of oxic and anoxic conditions on N-cycle processes in AM and ECM soils, and what environmental variables best explain N fluxes in AM and ECM forests? In this study, we used metagenomic analyses and microcosm experiments to investigate the potential for gaseous emissions of nitrogen oxides in AM- and ECM-dominated soils as well as along a gradient of AM to ECM soils throughout the eastern United States. Additionally, the response of key microbial transcripts coding for enzymes AMO, NIR, and NOS in AM- and ECM-dominated plots were analyzed by reverse transcription quantitative PCR (RT-qPCR). We hypothesized that (a) forests with more “open” N cycles (e.g., AM-dominated stands) contain microbial communities with greater numbers of N-cycling taxa and genes that are specifically related to the production of volatile nitrogen oxides, (b) anoxic soil conditions lead to significant increases in nitrogen oxide production and transcript copy numbers of denitrification genes in both AM and ECM soil; however, fluxes will be higher in AM soil relative to ECM soil, and (c) the

combined effects of N-cycle process rates and the relative abundance of N-cycle taxa will explain a significant amount of variation in the peak flux of soil  $\text{NO}_y$  and  $\text{N}_2\text{O}$ .

## 2 | MATERIALS AND METHODS

### 2.1 | Site description

Soils were collected in August 2017 from eight AM- and eight ECM-dominated plots (dominance implies >85% of the basal area of the plot) at the Indiana University Research and Teaching Preserve. This site will herein be referred to as “Moore's Creek.” Each plot at Moore's Creek was 20 m × 20 m. Additionally, soil was sampled in the summer of 2019 from a 54-plot AM to ECM gradient throughout the eastern United States—herein referred to as “gradient plots.” The gradient plots consisted of six sites, each containing nine 20 m × 20 m plots that varied the relative proportion of AM and ECM trees (e.g., from 0% to 100% AM/ECM tree abundance at each site). Gradient plots were located within research forests of the Smithsonian ForestGEO network (<https://forestgeo.si.edu/sites-all>). For both Moore's Creek and the gradient plots, trees were categorized by mycorrhizal association, and the percent of ECM trees (based on basal area) was determined according to Phillips et al. (2013). Site locations for plots used in this study can be found in Figure 2. Dominant soil orders in this study are inceptisols [Moore's Creek (MC) and Lilly Dickey Woods (LDW)], alfisols [Smithsonian Conservation Biology

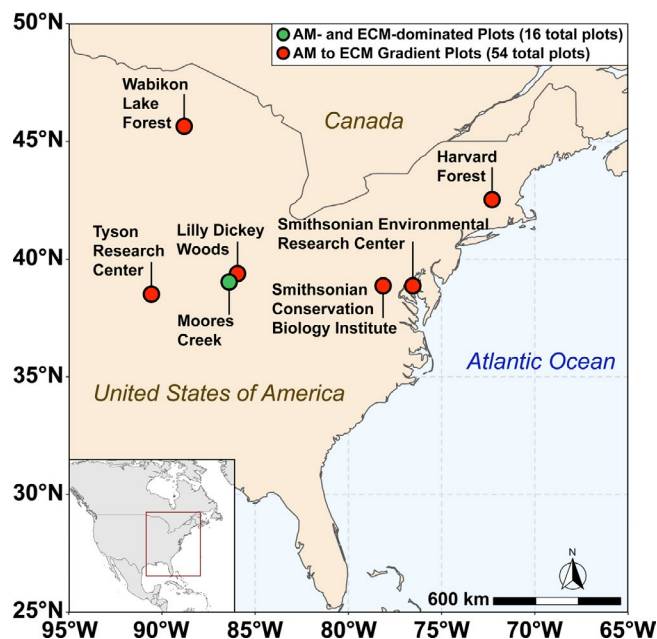


**FIGURE 2** Map of sampling locations across the eastern United States used in this study. The green dot indicates Moore's Creek where AM and ECM dominated plots are located while the red dots indicate sites associated with the 54-plot gradient. The Moore's Creek site contains 16 total plots (8-AM and 8-ECM dominated) while each site in the 54-plot gradient contains nine plots of varying AM/ECM composition

Institute (SCBI)], ultisols [Smithsonian Environmental Research Center (SERC)], spodosols [Harvard Forest (HF) and Wabikon Lake Forest (WLF)].

## 2.2 | Soil sampling

Within each plot (both Moores Creek and gradient plots), five soil cores (5.08 cm diameter) were collected at 0–5 cm. These individual soil cores were pooled by plot to increase mass and reduce environmental heterogeneity, resulting in 16 composited samples for Moores Creek and 54 composited samples for the gradient plots. From each composited sample, approximately 5 g of soil was immediately subsampled for molecular analysis and suspended in a preservation buffer (DNA/RNA Shield, Zymo Research), then shipped back to Indiana University whereupon the preservation buffer was removed, and soil was stored at  $-80^{\circ}\text{C}$ . The remaining composited sample was transported on ice packs to Indiana University where a 40 g aliquot of soil was dried at  $105^{\circ}\text{C}$  for gravimetric moisture and a 25 g aliquot was air-dried for soil pH analysis. The remaining field-moist soil was passed through a 2 mm sieve to further homogenize the soil, and to remove large organic matter fragments and rocks. Sieved soil was then stored at  $4^{\circ}\text{C}$  until further analysis.

## 2.3 | Overview of laboratory analyses

Soils from both Moores Creek and the gradient plots were analyzed for a common suite of physicochemical properties, including soil carbon and nitrogen content, soil pH, net nitrogen mineralization rate, and net nitrification rate. Gas fluxes ( $\text{CO}_2$ ,  $\text{NO}_y$  and  $\text{N}_2\text{O}$ ) were also analyzed for both sets of soils using microcosm incubations. Additionally, concentrations of oxalate-extractable iron and particle size analysis were analyzed for gradient plot soil. These physicochemical properties and gas flux measurements were used primarily to explore *hypothesis 1* and 3, where we define gas fluxes in relation to microbial community composition and which soil factors explain the majority of variation in  $\text{NO}_y$  and  $\text{N}_2\text{O}$  flux. DNA extracted from both Moores Creek and gradient plot soil was subjected to shotgun metagenomic sequencing; however, sequencing depth differed between the two groupings. Moores Creek soil DNA was used for deep shotgun sequencing (200 million reads per sample) whereas gradient plot soil DNA was used for a shallower analysis (12 million reads per sample). Both of these datasets were used to address *hypothesis 1* and 3. Moores Creek sieved soil was used to determine the relative influence of oxic and anoxic conditions on AM and ECM soil; specifically, the N-cycle microbial response, N-cycle rates, and fluxes of N gases. This set of experiments addresses *hypothesis 2* where we predict that anoxic conditions will stimulate N-cycle processes in AM soil more so than ECM soil. Detailed procedures are noted in the subsequent paragraphs.

## 2.4 | Soil physicochemical analysis

Soil pH was measured using an Orion pH meter (ThermoFisher Scientific, Waltham, MA, USA) on a 1:2 solution of air-dried soil in a 0.01 M  $\text{CaCl}_2$  solution. A 40 g sample of soil was dried at  $105^{\circ}\text{C}$  for 48 hr to calculate bulk density and gravimetric water content (GWC) as described in Mushinski et al. (2019). Ten grams of sieved soil was dried at  $60^{\circ}\text{C}$  for 48 hr, ground to a powder, and analyzed for soil total carbon (TC) and nitrogen (TN) using a Costech ECS 4010 elemental analyzer (Costech Analytical Technologies Inc.). Nitrate ( $\text{NO}_3^-$ ) pools were quantified from 4 g of sieved, field-moist soil with 15 ml of 2 M KCl within 36 hr of soil being taken from the ground and analyzed using a Lachat QuikChem 8000 Flow Injection Analyzer (Lachat Instruments). Total net nitrification and mineralization rates were calculated as the accumulation or depletion of inorganic N (mineralization:  $\text{NH}_4^+ + \text{NO}_3^-$ ; nitrification:  $\text{NO}_3^-$ ) over the course of a 14 day incubation. Soil texture was determined using a standard hydrometer procedure (Ulmer et al., 1994). Some plots had extremely high organic matter content in 0–5 cm depth increments, so plot level soil texture was derived from 5 to 15 cm increments. We quantified oxalate-extractable Al and Fe pools in all soil samples as an index of poorly crystalline Al- and Fe-oxides (Schwertmann, 1973); specifically, 0.40 g air dried pulverized soil was suspended in 40 ml 0.2 M ammonium-oxalate at pH 3.0 in the dark for 4 hr, gravity filtered, and analyzed with an atomic-absorption spectrometer (AAAnalyst 800, Perkin Elmer), using an acetylene flame and a graphite furnace for the atomization of Fe and Al, respectively.

## 2.5 | Measurement of soil gas fluxes under oxic conditions

All soils (normalized to 40% gravimetric water content) were preincubated in 100 mm diameter polystyrene petri dishes, in the dark for 24 hr at  $20^{\circ}\text{C}$ . Following soil preincubation, the petri dishes were loaded into 2 L glass jars, herein referred to as *chambers*, which were capped with polytetrafluoroethylene (PTFE) lids containing PTFE inlet and outlet ports. All glass and polystyrene surfaces were coated with an inert perfluorinated polymer film (Fluoropel PFC 801A, Cytonix Corp.) and Teflon tubing and PTFE fittings were used to reduce adsorption of reactive nitrogen oxides that could interfere with measurements. During incubation, the flux chambers were covered in black cloth to prevent photochemical conversions of reactive nitrogen oxides on soil surfaces.

Each experiment utilized five flux chambers; one contained an empty petri dish to act as the blank and four contained a petri dish with soil. During the course of the incubation, ultrapure zero-air was continuously flowed through a 5 Å molecular sieve and into a six-way PTFE manifold, delivering a continuous flow through each chamber [2 L/min, 1 atm, 0% relative humidity (RH)]. A solenoid array controlled by a microprocessor (R2 Series, OPTO 22) selectively sampled the outflow of gas from each of the chambers during their measurement period over the course of the 48 hr experiment cycle.

Gas flow from each soil-containing chamber was selectively sampled continuously for 10 min each hour, whereupon concentrations of CO<sub>2</sub>, N<sub>2</sub>O, NO, NO<sub>2</sub>, and HONO were analyzed. Measurements of the blank chamber flanked each soil measurement time period and were averaged over the course of each hour to determine background trace gas concentrations used in flux calculations.

Nitric oxide fluxes were measured using a modified chemiluminescence NO<sub>x</sub> analyzer (Air Quality Design, Inc.). The chemiluminescence instrument was equipped with a photolytic cell containing two LEDs with peak wavelengths at 385 and 395 nm. This allowed for the measurement of nitrogen dioxide (NO<sub>2</sub>) and nitrous acid (HONO) fluxes through differential photolysis (Reed et al., 2016). N<sub>2</sub>O fluxes were measured using an LGR ICOS (off-axis integrated cavity output spectroscopy) N<sub>2</sub>O/CO Analyzer (Los Gatos Research Inc.). Soil water content was calculated from air moisture concentration using linear regression of known gravimetric water content (GWC) at time 0 and 48 hr. Specifically, water vapor concentration of each chamber was regressed against actual GWC at time 0 hr (40% GWC) and 48 hr (0% GWC) to define an equation for GWC estimation based on water vapor. The equation was verified by measuring GWC at various time points between 0 and 48 hr. Carbon dioxide fluxes were measured using a LI-COR CO<sub>2</sub>/H<sub>2</sub>O analyzer (LI-840 A, LI-COR Inc.) and were used as a proxy for microbial respiration.

To calculate flux, concentrations of CO<sub>2</sub>, N<sub>2</sub>O, NO, NO<sub>2</sub>, and HONO were compared to a blank chamber using Equation (1).

$$\text{Flux} = \frac{1}{\tau} \times \frac{F_{\text{tot}} (C_{\text{soil}} - C_{\text{blank}})}{m_{\text{soil}}} \quad (1)$$

In Equation (1),  $\tau$  is the residence time of gas in the chamber,  $F_{\text{tot}}$  is the flow of the carrier gas,  $m_{\text{soil}}$  is the mass of soil, and  $C_{\text{soil}}$  and  $C_{\text{blank}}$  are the concentrations of analyte gas measured in the soil-containing and blank chambers, respectively. Positive fluxes describe net transfer of gases from soil to air (outgassing), while negative fluxes represent net transfer from air to soil (i.e., deposition or consumption). Flux data used for regression analysis were the peak flux value from each 48 hr experiment. NO<sub>y</sub> fluxes are defined as the combined fluxes of NO, NO<sub>2</sub>, and HONO.

## 2.6 | DNA extraction, shotgun sequencing, and metagenomic analysis

Moore's Creek soil was used for deep shotgun sequencing (200 million reads per sample) and subsequent metagenomic analysis. This depth of sequencing has been shown to provide accurate representation of the relative counts of genes for a given sample (Gweon et al., 2019). For all 16 samples, soil DNA was extracted from 0.3 to 0.4 g field-moist soil using a DNeasy PowerSoil Kit (Qiagen) and then six of the extracts were selected for downstream analysis using a random number generator. The purity of subsampled DNA extracts was measured using an Epoch microplate spectrophotometer (BioTek) and monitoring the absorbance ( $A_{\lambda}$ ) at  $\lambda = 260$  and 280 nm. Mean  $A_{260}/A_{280}$  ratios were

$1.94 \pm 0.04$  (mean  $\pm$  SD), indicating that protein and/or residual reagent contamination was minimal. Extracts were further verified by gel electrophoresis where no RNA bands were observed. Roughly 3  $\mu$ g of extracted DNA per sample was then sent to the DOE Joint Genome Institute (<https://jgi.doe.gov/>) for library preparation and shotgun sequencing on an Illumina NovaSeq 6000. Resulting raw Illumina reads were trimmed, quality filtered, and corrected using BFC (version r181) with the following options: `-1 -s 10g -k 21 -t 10` (Li, 2015). Reads were then assembled using SPAdes assembler 3.12.0 using the following options: `-m 2000--only assembler -k 33,55,77,99,127--meta -t 32` (Nurk et al., 2017). The entire filtered read set was mapped to the final assembly and coverage information generated using bbmap (version 38.22) using default parameters except `ambiguous = random` (<https://bbtools.jgi.doe.gov/>). The version of the processing pipeline was *jgi\_meta\_run.py* (version 2.0.1). The assembly pipeline resulted in  $1.95 \times 10^8$  aligned reads per sample with no significant difference between AM and ECM samples. Aligned reads were then subjected to the IMG/M pipeline where estimated gene copies associated with N-cycle activity within the Kegg Pathway (KO) database (<https://www.genome.jp/kegg/pathway.html>) were quantified. Estimated gene copy numbers were calculated as the number of genes multiplied by the average coverage of the contigs, on which these genes were predicted (Huntemann et al., 2016). Table S1 defines the specific KO associated with this analysis. Statistical differences between the number of N-cycle genes within AM and ECM metagenomes was assessed using Fisher's exact test.

N-cycle taxa distribution and functional potential was analyzed using DNA from the gradient plots. This was done to determine if N-cycle microbial trends seen in AM- and ECM-dominated plots were consistent across a large spatial gradient. Soil DNA from 54 plots of varying AM and ECM aboveground composition was extracted and quality-checked using the same methods mentioned above. Shotgun sequencing of extracted DNA took place at Indiana University's Center for Genomics and Bioinformatics (<https://cgb.indiana.edu/>) on an Illumina Hi-Seq platform, resulting in  $1.16 \times 10^7$  reads per sample and a mean quality score (Q-score) of  $34.6 \pm 0.1$  (mean  $\pm$  SD). Raw FASTQ files were analyzed using the MG-RAST pipeline where they were initially dereplicated to remove sequence artifacts (Gomez-Alvarez et al., 2009), screened to remove contaminant reads (Langmead et al., 2009), and trimmed to remove low-quality sequences using DynamicTrim at a minimum phred score of 15 (Cox et al., 2010). Resulting reads were taxonomically and functionally annotated against NCBI's RefSeq and KEGG's KO database, respectively. Data were further screened to include only N-cycle genes (KO) and associated taxa. N-cycle reads were normalized as a relative abundance value per the total number of N-cycle functional or taxonomic reads per sample.

## 2.7 | AM and ECM soil response to anoxic conditions

Using Moore's Creek soil, two analytical aliquots per sample (30 g) were placed in petri dishes and normalized to 40% GWC, which



corresponded  $68 \pm 16\%$  water filled pore space (WFPS). Samples were then pre-incubated in the dark at  $23^\circ\text{C}$  for 24 hr. Following pre-incubation, the first analytical replicate was placed into a sampling chamber, noted previously, whereupon ultrapure zero-air was continuously flowed throughout the chamber (2 L/min, 1 atm, 0% relative humidity) for 24 hr and concentrations of  $\text{CO}_2$ ,  $\text{N}_2\text{O}$ , and  $\text{NO}$  were continuously quantified from the outflow of gas. The second analytical replicate was placed in the same sampling chamber, but instead of air, ultrapure  $\text{N}_2$  ( $>99\% \text{N}_2$ ) was flowed through the system for 24 hr to simulate anoxic conditions. Measurements of gases from the anoxic replicate were performed in an identical manner to the oxic replicate. By the end of the experiment, all soils had reached  $22 \pm 3\%$  GWC. To calculate flux, concentrations of  $\text{CO}_2$ ,  $\text{N}_2\text{O}$ , and  $\text{NO}$  for the oxic and anoxic samples were compared to a blank chamber using Equation (1).

Net nitrification was also assessed under oxic and anoxic conditions. Specifically, 10 g of sieved, field fresh Moores Creek soil was weighed out, in duplicate, into 125 ml Wheaton bottles and capped with airtight butyl stoppers. One replicate (oxic) was flushed with ultra-pure air (20%  $\text{O}_2$ , 80%  $\text{N}_2$ ) for  $\sim 1$  min, while air from the other replicate was evacuated and replaced with helium (anoxic). Fresh air or helium was flushed through the incubations every 24 hr; field-level soil moisture was sustained throughout the experiment. Samples were incubated in the dark for 14 days and then soil was extracted with 25 ml of 2 M KCl, whereupon  $\text{NO}_3^-$  was quantified as noted previously.

To determine microbial N-cycle gene expression under different levels of oxygen availability, AM- and ECM-dominated soils from Moores Creek were incubated under different headspace atmospheres [oxic: ultra-pure air (20%  $\text{O}_2$ , 80%  $\text{N}_2$ ) or anoxic: helium (100% He)] for 8 and 24 hr. These time points were selected because they corresponded to the observed peak flux (8 hr) and the end of incubation (24 hr) for the gas flux experiment. Specifically, four analytical replicates (10 g) of each soil were placed in 125 ml Wheaton bottles. Two of the replicates were flushed with ultra-pure air, while the other two were flushed with helium. Soils were then incubated in the dark for the allotted time. At 8 hr after the initiation of the experiment, one oxic and one anoxic replicate were destructively sampled and  $\sim 0.5$  g soil was used for RNA extraction. This was also done at 24 hr after the initiation of the incubation. Soil RNA was extracted using the RNeasy PowerSoil Total RNA Kit (Qiagen) and further purified with the RNase-Free DNase Set (Qiagen). To quantify transcript abundance, cDNA was synthesized from the purified RNA with the QuantiTect Reverse Transcription Kit (Qiagen). Quantitative PCR (qPCR) of cDNA was performed using SsoAdvanced<sup>TM</sup> Universal SYBR<sup>®</sup> Green Supermix (Bio-Rad) on a QuantStudio 7 Flex Real-Time PCR System (ThermoFisher Scientific). Each plate included three analytical replicates per biological sample, synthetic oligonucleotide standards, and negative controls, also in triplicate. Copy numbers for each biological replicate were the average value of the three analytical replicates. Information on primers and thermocycling parameters is provided in Table S2.

## 2.8 | Statistical analyses

Soil physicochemical and gas flux data were analyzed using a mixed effects model where ectomycorrhizal tree abundance was the fixed effect and geographic location was the random effect. Data for N-cycle taxonomy from all soils were visualized using phylum percentage plots and differences in relative abundances were assessed using a two-factor ANOVA where independent variables included plot location and mycorrhizal category (Table S3). The mycorrhizal category included three levels grouped into AM-soil (plots  $\geq 85\%$  AM tree species), mixed-soil ( $<85\%$  AM and ECM tree species), and ECM-soil (plots  $\geq 85\%$  ECM tree species). Functional distribution of N-cycle genes was visualized using a non-metric multidimensional scaling (NMDS) plot, based on normalized Bray-Curtis distance matrices, where individual genes were grouped into process groupings. Significant physicochemical properties ( $p < .05$ ) were included as vectors on the NMDS. All analyses were done in R, using the *anova\_test* package for ANOVA and *vegan* for the NMDS. Significant differences among gas fluxes under oxic and anoxic conditions from Moores Creek soil were analyzed with a two-way repeated measures ANOVA, where stand-type (AM or ECM) and incubation headspace atmosphere [oxic: ultra-pure air (20%  $\text{O}_2$ , 80%  $\text{N}_2$ ) or anoxic: dinitrogen ( $>99\% \text{N}_2$ )] were fixed effects and incubation time (each hour for gas flux) was included as a repeated measure using the *anova\_test* function in R and visualized using OriginPro 2018. Transcript copy number were analyzed with the same two-way ANOVA procedure noted above. To assess the relative importance of vegetation composition, soil physicochemical properties, N-cycle process rates, and N-cycle microbes on peak flux values of  $\text{N}_2\text{O}$  and  $\text{NO}_y$ , we used a mixed effects model where the abundance of ECM trees, soil C:N, soil pH, percent clay, oxalate extractable iron, and aluminum, the relative abundance of N fixers, nitrifiers, and denitrifiers were fixed effects and geographic location (sampling sites) were random effects. This analysis was done with the *lme4* package and visualized with the *sjPlot* package, all in R.

## 3 | RESULTS

### 3.1 | Metagenomic analysis

Within gradient plot soil, the N-cycle community accounted for an average of 0.37% of all sequencing reads. Of the taxa with N-cycle capability, Proteobacteria, Actinobacteria, and Acidobacteria were dominant, with the Proteobacteria accounting for  $70 \pm 6\%$  (mean  $\pm$  SD) of the total N-cycle community across all soils (Figure 3a). Of the N-cycling Proteobacteria, genera such as *Sorangium*, *Shewanella*, and *Ralstonia* were quite abundant in AM soil, and decreased in abundance as ECM tree abundance increased (Figure S1). In contrast, other dominant genera including *Mycobacterium* (Actinobacteria) and *Acidobacter* (Acidobacteria) increased significantly as ECM tree abundance increased (Figure S1). N-cycle fungi and archaea

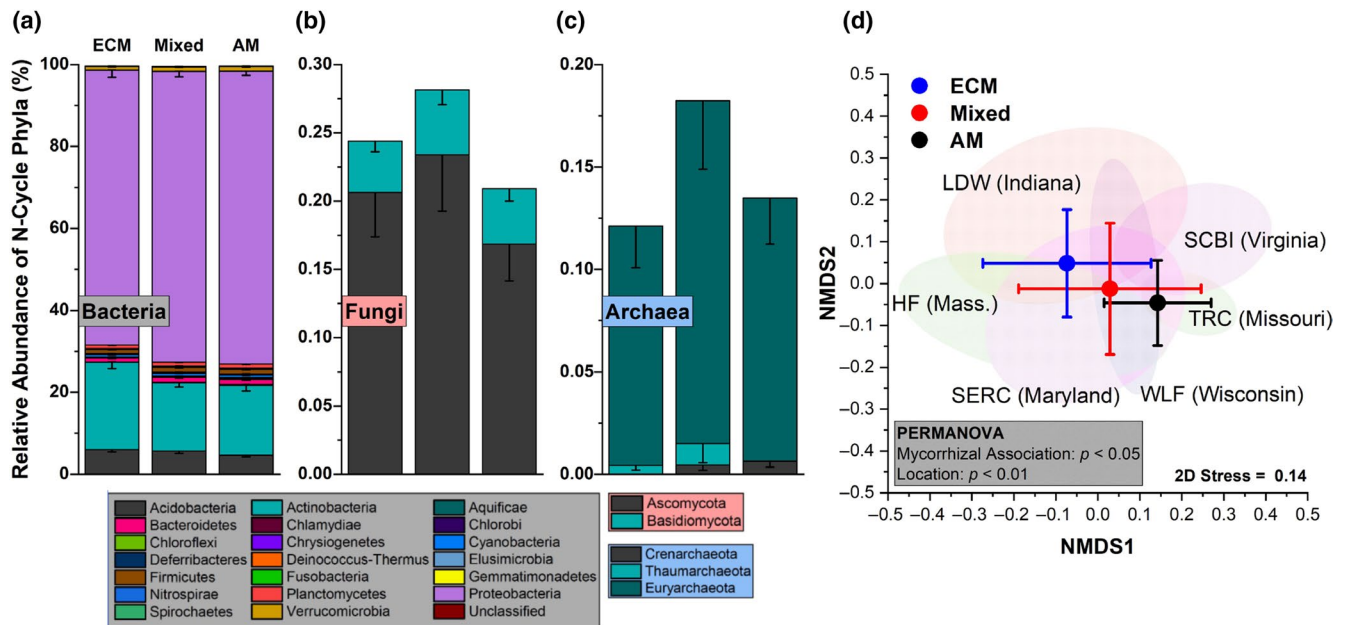


**FIGURE 3** Relative abundance profiles for nitrogen cycling bacteria (a), fungi (b), and archaea (c) from the 54-plot AM to ECM gradient. This subset of phyla account for 0.37% of all sequencing reads. Each segment is the mean relative abundance and the error bars are standard error. The mycorrhizal category included three levels grouped into AM-soil (plots  $\geq 85\%$  AM tree species), mixed-soil ( $<85\%$  AM and ECM tree species), and ECM-soil (plots  $\geq 85\%$  ECM tree species). Sample size for ECM = 25, Mixed = 20, AM = 21. (d) Non-metric multidimensional scaling plot for the distribution of N-cycle taxa in relation to mycorrhizal type as well as ellipses (95%) for sampling sites

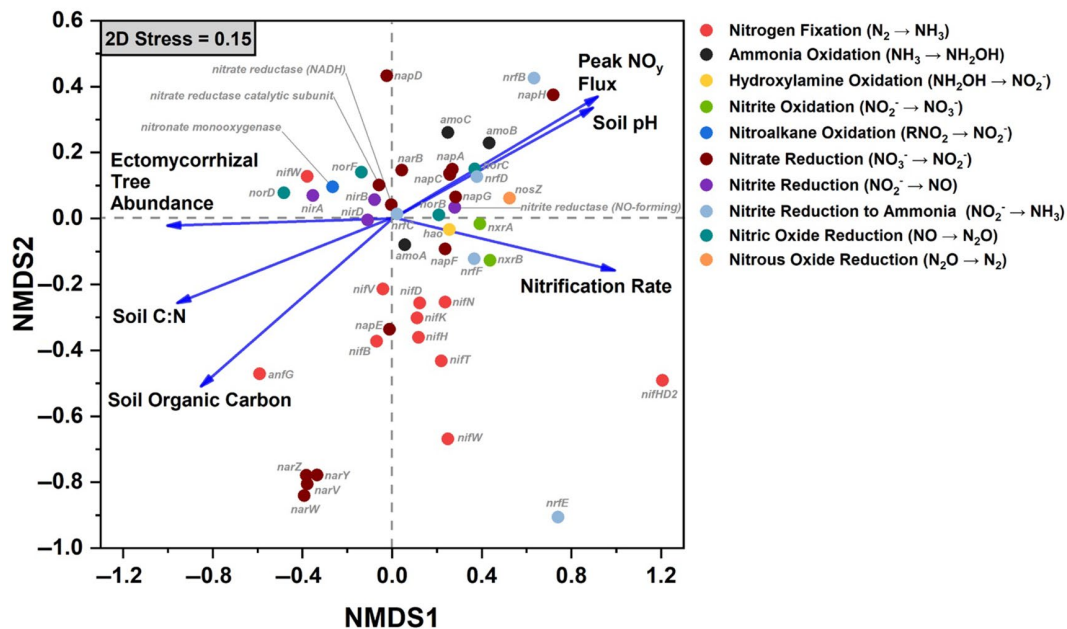


**FIGURE 4** Non-metric multidimensional scaling (NMDS) plot showing the distribution of nitrogen cycling genes (based on relative abundance values) and significant environmental properties as vectors ( $p < .05$ ). Data for the NMDS are taken from the 54-plot gradient

accounted for less than one percent of the total N-cycle community, and were influenced by sample location (Figure 3b,c). The N-cycling Crenarcheota, were lower in the ECM soil (AM + Mixed versus ECM:  $p < .05$ ). The overall structure of the N-cycle community was significantly influenced by both dominant mycorrhizal classification of aboveground tree communities and site location (Figure 3d). N-cycle community metrics were also influenced by tree assemblage with

Simpson's index, Shannon's index, the number of N-cycle taxa, and Pielou's evenness all decreasing as the abundance of ECM trees increased (Figure S2). Using NMDS, we assessed the relationship between the relative abundance of N-cycle genes and soil physicochemical factors within the 54-plot gradient (Figure 4). We found that peak NO<sub>y</sub> flux from soil microcosms and soil pH were linked to higher abundances of genes in the *amo*, *nap*, *nor*, and *nrf* operons.

Net nitrification rate was linked closely to the positive NMDS axis 1, along with nitrification genes *amoA*, *hao*, and *nirAB*. Ectomycorrhizal tree abundance was almost exclusively correlated to the negative NMDS axis 1, which also correlated with NIR and NOR genes. The two other significant vectors (soil C:N and soil organic carbon content) were not closely associated with any genes other than the nitrogen fixation gene, *anfG*.

Deep shotgun sequencing for Moores Creek soil showed AM soil possessed greater potential for all N-cycle transformations except nitrogen fixation, which was relatively low in both AM and ECM soil (Figure 5). The highest estimated copy number was associated with nitrite/nitrate oxidation and reduction pathways, with *nasA* (assimilatory nitrate reductase catalytic subunit) accounting for 41% and 73% of all reported N-cycle genes in AM- and ECM-dominated soil, respectively (Table S1, Figure S3). Analysis of N-cycle gene distribution for Moores Creek soil is consistent with the gradient plot soil, showing the relative proportion of genes associated with hydroxylamine oxidation, nitrite reduction, nitrate reduction, nitric oxide reduction, and nitrous oxide reduction increased from ECM to AM (Figure 6). Conversely, the relative abundance of N-conservation genes associated with nitrite reduction (*nirA*), nitrate reduction (*nasA*), and nitroalkane oxidation increased in conjunction with increasing ECM tree abundance for gradient plot soils (Figure 6).

### 3.2 | NO<sub>y</sub> and N<sub>2</sub>O flux

Across seven sites, peak NO<sub>y</sub> flux decreased linearly from an average of 3.5 to 1.5 ng-N g-soil<sup>-1</sup> hr<sup>-1</sup> as the percentage of ECM trees

increased from 0% to 100% (Figure 7a). ECM tree abundance accounted for 33% of variation in NO<sub>y</sub> flux (marginal R<sup>2</sup>), while ECM tree abundance combined with the random site factor accounted for 56% of NO<sub>y</sub> flux variability (conditional R<sup>2</sup>). Peak N<sub>2</sub>O flux ranged from 0.5 to -3 ng-N g-soil<sup>-1</sup> hr<sup>-1</sup>, did not vary by site, and did not correlate to changes in ECM tree abundance (Figure 7b).

### 3.3 | Oxidic and anoxic microcosms

Fourteen-day incubations of AM- and ECM-dominated soil (Moores Creek soil) under differing incubation headspace atmospheres (e.g., oxic vs. anoxic) altered concentrations of aqueous oxidized nitrogen (Figure S4). Concentrations of NO<sub>3</sub><sup>-</sup> were always greater in AM soil than those in ECM soil. For AM soil, oxic incubation led to an increase of 9.3 µg-N g-soil<sup>-1</sup> (+98%) relative to field-levels ( $p < .001$ ) while anoxic incubation resulted in a decrease of 4.0 µg-N g-soil<sup>-1</sup> (-58%;  $p < .1$ ). In ECM soil, initial levels of NO<sub>3</sub><sup>-</sup> were 8.6 µg-N g-soil<sup>-1</sup> lower than the AM soil. Oxic and anoxic incubations of ECM soil led to a decrease of 0.8 and 0.9 µg-N g-soil<sup>-1</sup>, which represents a -89% and -95% change, respectively ( $p < .001$ ).

Within Moores Creek samples, gas fluxes from both AM and ECM soil were heavily influenced by water content, and generally decreased as soil dried (Figure 8). CO<sub>2</sub> flux (microbial respiration) did not vary in response to incubation atmosphere conditions nor mycorrhizal soil type, which is consistent with what was observed when peak CO<sub>2</sub> flux from the AM to ECM gradient plots was analyzed in response to ECM abundance (Figure S5). For N<sub>2</sub>O and NO, higher values under anoxic conditions were observed for the AM soil (NO: 145.4 ± 75.5 ng-N g-soil<sup>-1</sup> hr<sup>-1</sup>; N<sub>2</sub>O: 31.8 ± 30.2 ng-N g-soil<sup>-1</sup> hr<sup>-1</sup>). ECM soil fluxes of NO<sub>y</sub> and N<sub>2</sub>O were extremely low and differences between oxic and anoxic conditions were negligible (Figure 8). NO flux in AM soil peaked at 13 and 7 hr under oxic and anoxic conditions, respectively. In ECM soil, flux decreased linearly from 0.32 to 0.12 ng-N<sub>NO</sub> g-soil<sup>-1</sup> hr<sup>-1</sup> under oxic conditions and from 8.35 to <0.1 ng-N<sub>NO</sub> g-soil<sup>-1</sup> hr<sup>-1</sup> under anoxic conditions. Only AM soil produced a definitive peak N<sub>2</sub>O flux, which occurred at 5 hr under anoxic conditions (44.0 ng-N<sub>N2O</sub> g-soil<sup>-1</sup> hr<sup>-1</sup>).

Using RT-qPCR, we determined that transcript abundance of AOA and AOB *amoA* was higher under oxic conditions for Moores Creek soil and tended to decrease with time (Figure S6). For AOA *amoA*, the average number of transcripts was 72% higher in AM soil relative to ECM soil ( $p < .001$ ), while AOB *amoA* transcript numbers were 177% higher in AM soil ( $p < .001$ ). Regardless of soil type or oxygen availability, denitrification transcript abundance followed *nosZ* (Clade I) > *nirK* > *nirS*. For AM soil, denitrification transcripts were higher under anoxic conditions; however, in ECM soil, there was no difference in transcript copies for the key N-cycle genes between oxic and anoxic incubations. Incubation time (i.e., 8 and 24 hr) influenced *nirK* and *nosZ* (Clade I) where 8 hr < 24 hr, but not *nirS*. Many of the transcript levels for ECM soil were below detection limits.

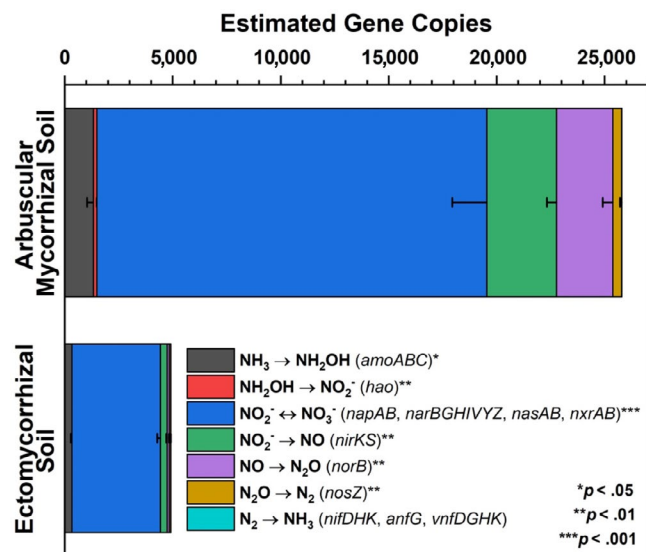


**FIGURE 5** Estimated gene copies of key nitrogen cycle genes defined from metagenomic sequencing. Asterisks indicate level of significant difference between dominant mycorrhizal soil types taken from AM- and ECM-dominated soil (Moores Creek). Estimated gene copy numbers were calculated as the number of genes multiplied by the average coverage of the contigs, on which these genes were predicted. Error bars indicate standard error of three replicates



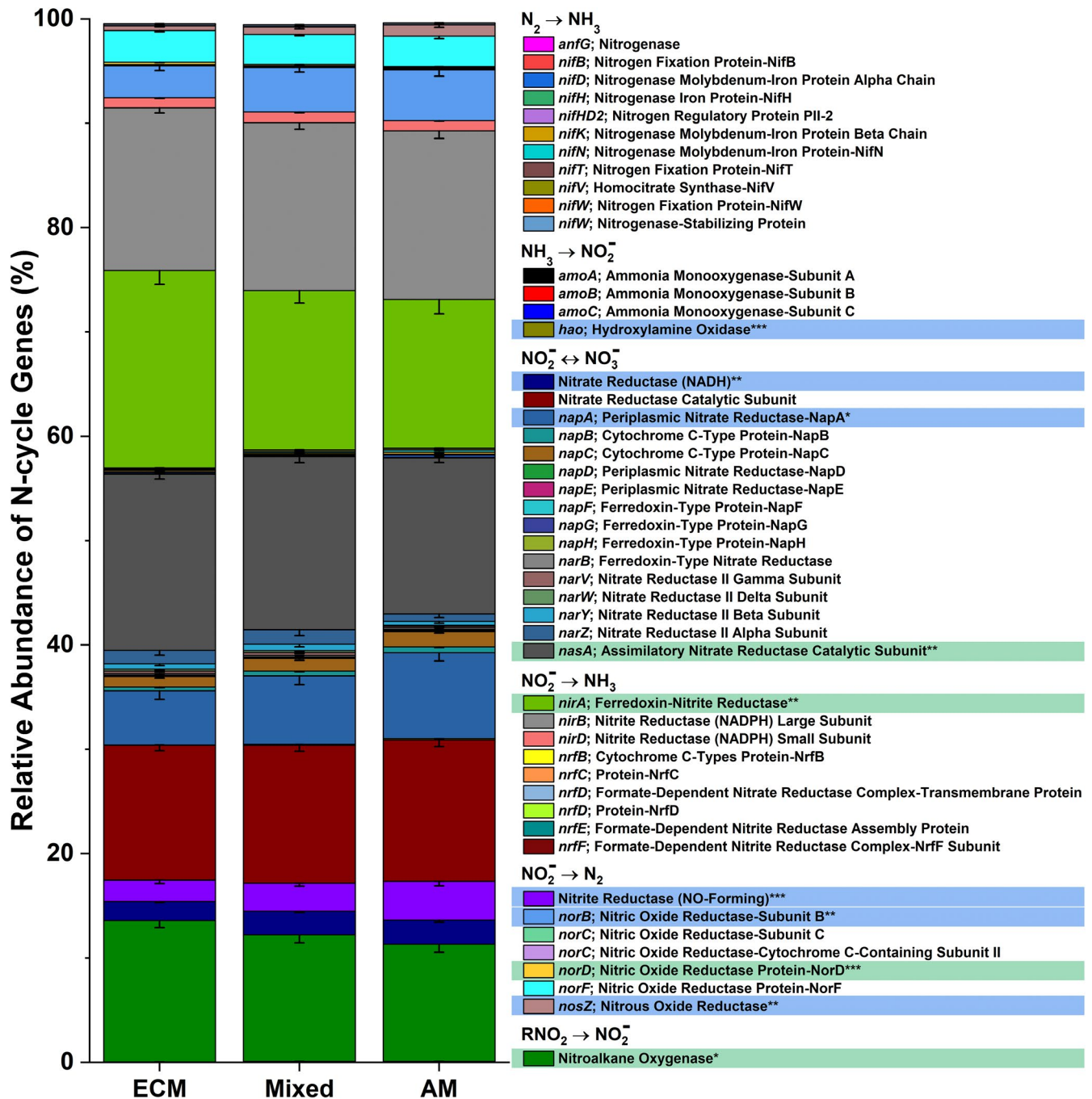


**FIGURE 6** The relative abundance of nitrogen cycle genes across the 54-plot gradient. The mycorrhizal category included three levels grouped into AM-soil (plots  $\geq 85\%$  AM tree species), mixed-soil ( $<85\%$  AM and ECM tree species), and ECM-soil (plots  $\geq 85\%$  ECM tree species). Sample size for ECM = 25, Mixed = 20, AM = 21. Genes highlighted blue are significantly more abundant in AM stands, while those highlighted in green are more abundant in ECM stands

### 3.4 | Mixed effects models—factors responsible for $NO_y$ and $N_2O$ flux

In gradient soil, fixed effects (ECM tree abundance, C:N, pH, percent clay, oxalate extractable iron and aluminum accounted, microbial respiration, net N mineralization, net nitrification, and the relative abundance of N fixers, nitrifiers, and denitrifiers) accounted for 18% and 38% of variation (marginal  $R^2$ ) for peak  $N_2O$  and  $NO_y$  flux,

respectively (Figure 9). This level of variance was significant for  $NO_y$  but not  $N_2O$  flux. Conditional  $R^2$  was 39% ( $N_2O$ ) and 80% ( $NO_y$ ), indicating that the random factor (geographic location) plays a large role in nitrogen oxide flux variation across a spatial gradient. For  $N_2O$  flux, soil C:N was the only factor with a significant effect size, while variables such as ECM tree abundance, percent clay, microbial respiration, net nitrogen mineralization, and net nitrification were significantly predictive of  $NO_y$  flux (Figure 9).

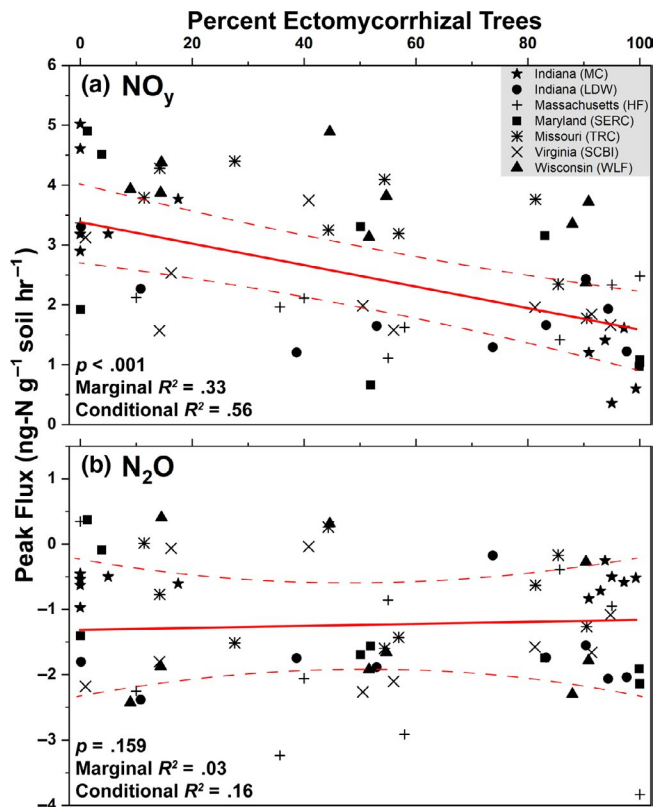


**FIGURE 7** Results from a linear mixed effects model where peak NO<sub>y</sub> (a) and N<sub>2</sub>O (b) flux were the response variables and the percent of ectomycorrhizal trees was the independent variable. Data are combined from both sets of sites (Moores Creek and gradient plots). Site location was assessed as a random effect. The solid red line is the regression equation and dashed lines represent the 95% confidence intervals. The  $p$ -values indicate the significance of the independent predictor (percent ectomycorrhizal trees) on peak fluxes of NO<sub>y</sub> and N<sub>2</sub>O. Peak fluxes were defined as the highest flux value over the course of the 48-hr incubation. Marginal  $R^2$  indicates the explained variability of gas fluxes solely on the effect of the independent predictor while the conditional  $R^2$  accounts for variation of the independent predictor and the random effect (site location)

## 4 | DISCUSSION

### 4.1 | Metagenomic analyses reveal greater potential for N-cycle activity in AM soil

The higher abundance of N-cycle genes such as *amoABC*, *hao*, and *nirAB* in AM-dominated soils are in agreement with previous studies showing that under oxic conditions, AM soils have greater rates of net nitrification (Midgley & Phillips, 2016; Mushinski et al., 2019; Phillips et al., 2013), which likely explains high rates of oxic NO<sub>y</sub> flux shown in AM soils (Figure 7). Estimated gene copy numbers for *norB* and *nosZ*, which code for nitric oxide reductase and nitrous oxide reductase, respectively, were both higher in AM-dominated soil (Figure 5) and the relative abundance of these same genes were in greater proportion in AM soil along the 54-plot gradient (Figure 6). This indicates that under reducing conditions, AM soil has

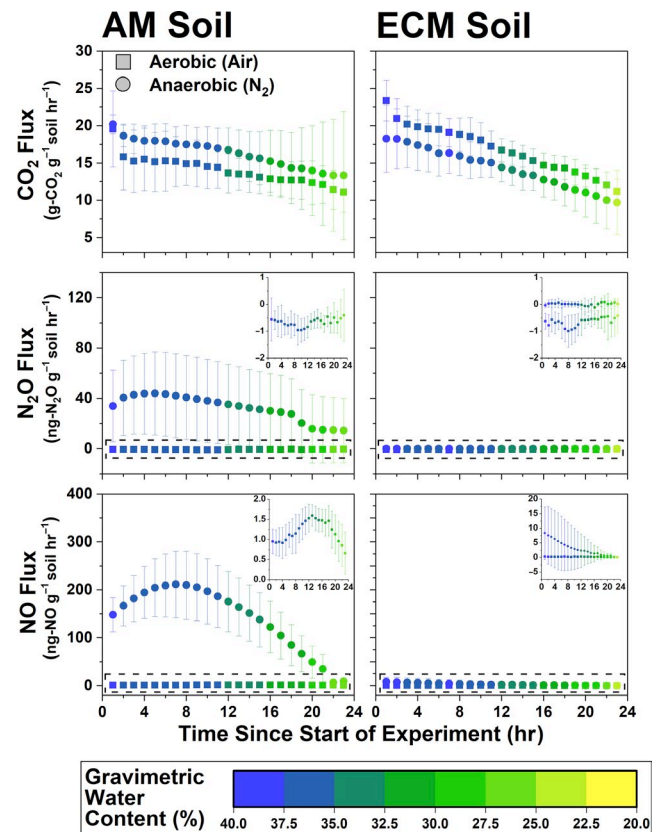


**FIGURE 8** Gas fluxes (CO<sub>2</sub>, N<sub>2</sub>O, and NO) for 24 hr incubations under oxic (ultra-pure air: 20% O<sub>2</sub>, 80% N<sub>2</sub>) and anoxic (>99% N<sub>2</sub>) conditions. Inset for fluxes shows finer resolution of data within dashed boxes. Soil used in this experiment is from AM- and ECM-dominated plots at Moores Creek. For each data series,  $N = 8$ .

the genomic potential for volatile nitrogen oxide flux to be much higher relative to ECM soil, which was verified by flux measurements conducted under anoxic conditions (Figure 8). *NasA* was by far the most abundant N-cycle gene in Moores Creek soil and was the third most abundant N-cycle gene in the gradient plots. *NasA* was also significantly more abundant in all ECM soils tested (Moores Creek and gradient soils). This gene codes for an assimilatory nitrate reductase catalytic subunit which reduces NO<sub>3</sub><sup>-</sup> to NO<sub>2</sub><sup>-</sup> and is associated with microbial uptake of NO<sub>3</sub><sup>-</sup>. The high estimated *nasA* copy numbers in Moores Creek soil indicate the importance of microbial uptake and conservation of oxidized N in these forests systems. Furthermore, the high proportion of *nasA* in ECM soil indicates high uptake and utilization of any free NO<sub>3</sub><sup>-</sup>, which may partially explain low concentrations of NO<sub>3</sub><sup>-</sup> in ECM soil. While AM soils also have high relative abundance of *nasA*, NO<sub>3</sub><sup>-</sup> uptake is likely supplemented by high rates of nitrification and ammonification, resulting in a very fast N cycle in AM soil.

AM-induced microbial stimulation coupled with higher litter quality and fast turnover rates may explain why genes associated with heterotrophic microbes such as denitrification are significantly higher in the AM soil (Figure 5), leading to higher fluxes of nitrogen oxide, specifically NO<sub>y</sub> (Figures 7, 8). AM soils throughout these sites (Craig et al., 2018; Midgley et al., 2015) and elsewhere (Craig et al., 2018; Keller & Phillips, 2019; Lin et al., 2017) have leaf litter layers of low lignin:N ratios (i.e., higher chemical quality). Given the well-established

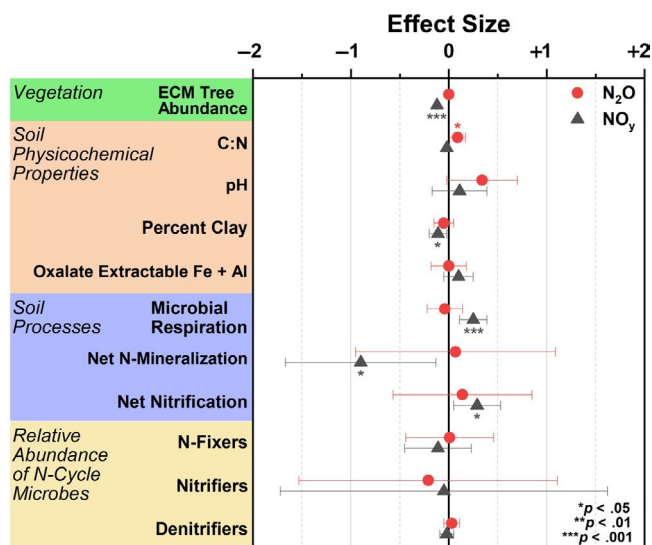


**FIGURE 9** Effect size from a linear mixed effects model where nitrogen oxide flux ( $\text{N}_2\text{O}$  or  $\text{NO}_y$ ) was the response variable and edaphic parameters including vegetation composition, soil physicochemical properties, soil processes, and the relative abundance of nitrogen cycling microbial guilds were fixed predictive variables. Data were used from the gradient plots. Geographic location was used as a random effect.  $R^2$  for  $\text{NO}_y$  was 0.38/0.80 (marginal  $R^2$ /conditional  $R^2$ ) and 0.18/0.39 for  $\text{N}_2\text{O}$ . Model intercepts:  $\text{NO}_y = 3.43 \pm 5.21$ ;  $\text{N}_2\text{O} = -5.45 \pm 6.32$

relationship between fast cycling litters and N availability in forests (Scott & Binkley, 1997), and the relationship between inorganic N pools and nitrification fluxes (Persson et al., 2000), we expect microbes responsible for accelerating the N cycle to be more common in AM soils. However, differences in the physiology and metabolism of mycorrhizal fungi may also contribute to the observed differences in microbial community composition between AM and ECM soils. Although ECM fungi possess hydrolytic capabilities that can result in the slow liberation of organic C and N from complex SOM (Kohler et al., 2015; Lindahl & Tunlid, 2015), AM fungi can release labile carbon into the hyphosphere, leading to greater stimulation of heterotrophic microbes (Herman et al., 2012; Kuzyakov, 2010; Paterson et al., 2016; Talbot et al., 2008), and possibly greater litter decay rates (Bunn et al., 2019). ECM fungi produce significant amounts of mycelium which may function as a large sink of inorganic N (Högberg & Högberg, 2002), possibly shaping the free-living N-cycle community in ECM soil toward more N conservation rather than processes leading to N loss such as nitrification and denitrification. Quantification of AM and ECM fungi within these soils would better elucidate the importance of these potential mechanisms.

It is unknown how differences in AM and ECM microbial communities influence precursory processes to nitrification, such as ammonification. Pools of ammonium were similar in AM- and ECM-dominated soil but rates of ammonium accumulation were significantly higher in ECM soil (Figure S7), indicating a potential bottleneck at the nitrification step. This may be a function of the higher acidity observed in ECM soil, which directly influences rates of nitrification

through the protonation of ammonia to ammonium ( $\text{NH}_4^+$ ,  $\text{p}K_a = 9.3$ ); this renders the substrate less available for nitrification and other downstream processes, inevitably selecting for lower abundances of ammonia oxidizers, as seen previously (Mushinski et al., 2019). Soil pH (which positively correlates with ECM tree abundance) can also influence N cycling by modifying microbial diversity. Less acidic AM soils support greater microbial diversity (Fierer & Jackson, 2006) and higher N-cycle potential (Figure S2; Figure 5)—heterotrophic microbes involved in mineralization are likely affected by soil pH in the same manner. Further inhibition may be mediated by the presence of litter-derived polyphenolic compounds, which tend to be more abundant in ECM soil (Subbarao et al., 2013). This nitrification bottleneck hypothesis is further supported by a supplemental experiment showing that when ECM soil is supplemented with inorganic N (nitrite) under anoxic conditions, increases in  $\text{N}_2\text{O}$  production and denitrification transcripts are observed (Figure S8). This indicates that ECM soil is inherently able to produce nitrogen oxides, but the process is repressed due to a lack of available substrate, likely as a result of the inhibition of nitrification.

## 4.2 | Oxygen availability alters N-cycle rates and microbial activity in AM soil

Variations in oxygen availability can drive dramatic changes in nitrogen oxide production by stimulating different groups of N-cycle microbes. We hypothesized that anoxic conditions would lead to greater emissions of nitrogen oxides for both AM and ECM soil, with AM soil producing significantly greater N-gas fluxes under anoxic conditions. Our results partially support this hypothesis; there was no significant response from ECM soil to anoxic conditions. Consistent with our hypothesis, AM soil produced more NO and  $\text{N}_2\text{O}$  relative to ECM soil (Figure 8)—likely a direct result of higher oxidized N availability and greater potential for denitrification. This observation agrees with a field-based study which showed that under poorly drained (partially anoxic) conditions, AM (maple) stands produced three to four times more  $\text{N}_2\text{O}$  relative to ECM (beech) stands (Ullah & Moore, 2011). The difference between anoxic and oxic NO and  $\text{N}_2\text{O}$  flux in AM soil was extremely large, relative to ECM soil. NO flux increased by roughly  $144 \text{ ng-N g-soil}^{-1} \text{ hr}^{-1}$  and  $\text{N}_2\text{O}$  flux increased by  $32 \text{ ng-N g-soil}^{-1} \text{ hr}^{-1}$  under anoxic conditions in AM soil, which was more than the 3 and  $0.8 \text{ ng-N g-soil}^{-1} \text{ hr}^{-1}$  increases in ECM soil. The lower flux levels for  $\text{N}_2\text{O}$  may be a result of greater  $\text{N}_2\text{O}$  to  $\text{N}_2$  conversion, a prediction that agrees with *nosZ* having high gene expression. Furthermore, at its highest flux value (i.e., at hour 8 of the incubation), the amount of N being lost from AM soil accounted for roughly 2% of the entire pool of  $\text{NO}_3^-$ . Soil transcript abundance of key N-cycle genes confirmed that observed fluxes were the result of biological processes where, under oxic conditions, nitrification transcripts (AOA and AOB *amoA*) were more abundant than denitrification transcripts (*nirS*, *nirK*, *nosZ*), and vice versa under anoxic conditions (Figure S6). It is also worth noting that AM forest soil may be inherently more anoxic due to AM fungi

promoting soil aggregation through the release of labile organic compounds (Wright et al., 1999).

The large discrepancy between AM and ECM soil nitrogen oxide flux has substantial implications for future forest dynamics. Even currently, individual AM trees in ECM-dominated forests likely produce soil hotspots of nitrogen oxide flux regardless of soil oxygen condition. Upland forest soils have generally been shown to be sources of  $N_2O$  and NO; however, the magnitude of this source depends on vegetation composition, geographic location, and previous land-use history (Butterbach-Bahl et al., 2013; Chapuis-Lardy et al., 2006; Pilegaard, 2013). Systems with highly conservative N-cycle dynamics, as seen in oak-hickory-beech (ECM) forests throughout the eastern United States, are presumed to contribute much less relative to adjacent agricultural systems; however, fast N-cycling AM forests have not been considered. It is likely that these forests do not naturally receive enough N inputs to compare to fluxes measured from major US crops such as corn (Decock, 2014) (0 to  $30 \text{ kg-N}_{N_2O} \text{ ha}^{-1} \text{ year}^{-1}$ ) and switchgrass (Ruan et al., 2016) (0 to  $6 \text{ kg-N}_{N_2O} \text{ ha}^{-1} \text{ year}^{-1}$ ), which typically receive large amounts of N fertilizer (up to  $200 \text{ kg-N}_{\text{fertilizer}} \text{ ha}^{-1} \text{ year}^{-1}$ ). For reference, temperate forests of the eastern United States are estimated to receive  $10\text{--}15 \text{ kg-N/ha}^{-1} \text{ year}^{-1}$  via atmospheric deposition (Schwede et al., 2018). However, our observation that anoxic soil conditions stimulate microbial denitrification and large increases in  $N_2O$  and NO flux for AM soil is noteworthy, especially in light of the increasing abundance of AM trees across much of the eastern United States (Jo et al., 2019). While it has typically been assumed that well-drained upland soils are completely oxic, 2%–9% of the pore volume can be anoxic, even when bulk soil  $O_2$  concentrations are high (Keiluweit et al., 2018). This indicates that in situ N gas fluxes from forest soils may be higher than what is currently assumed and should be compared to adjacent natural and managed ecosystems.

### 4.3 | Multiple factors influence the production of volatile nitrogen oxides in forest soil

Results from Figure 9 illustrate that reactive  $NO_y$  fluxes are best explained primarily by the relative abundance of ECM trees species and to a lesser degree, the percentage of clay and soil processes such as microbial respiration, net N mineralization, and net nitrification. Except for net nitrification, none of these factors were included in a previous study (Mushinski et al., 2019). The significant influences of ECM on  $NO_y$  flux is likely due to combined effects of ECM trees in lowering soil pH due to acidifying processes associated with litter decomposition. This in turn lowers the abundance of available ammonia, nitrifiers, and nitrification rates, which are all directly related to  $NO_y$  flux. It was surprising that soil clay content was a significant factor in this model due to its lack of correlation to ECM tree abundance (Figure S5); however, clay content is likely important in modulating oxic and anoxic conditions, soil porosity, and soil reactivity which may influence  $NO_y$  production (Kebede et al., 2016; Maharjan & Venterea, 2014). Furthermore, the amount of variance explained increased from 23% in the initial model

(Mushinski et al., 2019) to 39% for fixed effects only and 80% for fixed effects plus the influence of geographic location (mixed model, this paper). Note that the relative abundance of N-cycle microbes was not found to be a significant predictive variable for oxic  $NO_y$  fluxes. Mushinski et al. (2019) identified nitrifying microbes (AOA and AOB) as contributing 60%–70% to oxic  $NO_y$  flux from inhibitor assays; however, this was based on activity and not functional potential as shown here. RNA-based methods will likely provide better resolution on the contribution of specific microbial guilds. Considering the large flux differences in response to oxygen availability, similar analyses should be carried out to determine the factors responsible for anoxic flux of nitrogen oxides in these systems. The varied responses of  $N_2O$  and  $NO_y$  in these experiments is difficult to interpret—considering they are both products of nitrification and denitrification. However, it may stem from multiple factors including unknown abiotic chemistry, an extremely efficient conversion of  $N_2O$  to  $N_2$ , or simply a function of the microcosms used in this study—it remains to be seen whether the microcosm chambers yield the same results as in situ chamber flux measurements. Although, studies in grasslands suggest good agreement between the two methods (van Dijk et al., 2002).

### 4.4 | Synthesis

Changes in global climate and other disruptions such as atmospheric deposition of anthropogenic N are inducing shifts in the relative abundance of AM and ECM trees in temperate forests (Jo et al., 2019; Steidinger et al., 2019), with unknown consequences for biogeochemical cycling in these systems. Our study illustrates that the global change-induced vegetation shifts currently being observed throughout the eastern United States (Jo et al., 2019) may significantly alter the soil bacterial and archaeal N-cycling communities and have significant effects on atmospheric composition, especially in the wake of climate change. We hypothesized that forests with more “open” N cycles (e.g., AM-dominated stands) contain microbial communities with greater numbers of N-cycling taxa and genes that are specifically related to the production of volatile nitrogen oxides. Using forests throughout the eastern United States (Figure 2), we find support for this hypothesis: AM-dominated soils had microbial communities with a greater relative abundance of N-cycling genes. This in turn leads to greater metagenomic potential for ammonia oxidation, hydroxylamine oxidation, nitrite oxidation/reduction, nitrate reduction, nitric oxide reduction, and nitrous oxide reduction (Figure 5). Additionally, we observed mycorrhizal-based differences in the N-cycling bacterial consortia (Figure 3a–c), the structure of the N-cycle microbial community (Figure 3d) as well as a different proportional profile of N-cycle taxa and genes based on mycorrhizal association (Figure 6; Figure S3). The spatial variability of nitrogen oxide fluxes was also investigated. We found  $NO_y$  fluxes to be highest in AM soils across the eastern United States (Figure 7) and strongly correlated to the relative abundance of genes associated with nitrification and denitrification (Figure 4); however, the magnitude of flux was dependent on geographic location (mixed effects model). We also found support for our hypothesis



that anoxic conditions lead to equivalent or greater emissions of nitrogen oxides for both AM and ECM soil, with AM soil producing more  $N_2O$  and  $NO_y$  under anoxic conditions (Figure 8)—likely a direct result of higher N availability and greater microbial potential for denitrification. Furthermore, the low levels of inorganic nitrogen in ECM soil may serve as a bottleneck to nitrogen oxide production (Figure S4), which was supported by a positive  $N_2O$  response following addition of nitrite (Figure S8). Collectively, our results suggest that shifts in forest composition may have profound consequences for microbial communities involved in N cycling and the tendency of forest soil to modulate volatile nitrogen oxides. Furthermore, this study indicates that proliferation of AM species into ECM-dominated ecosystems throughout temperate forest regions may represent a major change in the soil N-cycle microbiome, possibly leading to ecosystem-scale altering of soil N-cycle process rates and high loss of soil N through volatilization, regardless of soil oxygen conditions.

## ACKNOWLEDGEMENTS

We thank John Poehlman, Jeremy Boshears, and colleagues in Indiana University Chemistry's Engineering and Technical Groups for help designing and building the automated chamber sampling system used in this study. We also thank Meghan Midgley for establishing the Moores Creek research plots at Indiana University's Research and Teaching Preserve (funded by Agriculture and Food Research Initiative Competitive Grant 2013-67011-21095 from the US Department of Agriculture National Institute of Food and Agriculture) as well as Laura Podzikowski, Mark Sheehan, Katilyn Beidler, and Elizabeth Huenupui for maintaining and fertilizing the Moores Creek plots since 2015. We also thank Edward Brzostek and his lab at West Virginia University for assistance in sampling the 54 gradient plots. Sequencing support was provided by the US Department of Energy Joint Genome Institute (JGI), a DOE Office of Science User Facility, which is supported by the Office of Science of the United States Department of Energy under Contract No. DE-AC02-05CH11231. We especially thank the staff at the JGI, including Nicole Shapiro and Natalia Ivanova for assistance with sequencing and bioinformatic analyses. We also thank Ayumi Hyodo and the Stable Isotopes for Biosphere Sciences laboratory at Texas A&M University for help with soil elemental analysis. Financial support for this study came from the US Department of Energy, Office of Science, Early Career Research Program from Subsurface Biogeochemical Research Program (Award DE-SC0014443 to J.D.R.). R.M.M. was supported by Indiana University's Integrated Program in the Environment and the O'Neill School of Public and Environmental Affairs as well as a postdoctoral fellowship from the US Department of Agriculture National Institute of Food and Agriculture (grant no. 2018-08037). Z.C.P. was supported by NSF Grant AGS-1352375. M.E.C. was supported by Oak Ridge National Laboratory, which is operated by UT-Battelle, LLC, under contract DE-AC05-00OR22725 with the United States Department of Energy. We also thank Peter Homyak and an anonymous reviewer for extremely helpful feedback.

## CONFLICT OF INTEREST

The authors claim no competing interests for this work.

## AUTHOR CONTRIBUTIONS

R.M.M. led the work; R.M.M., Z.C.P., J.D.R., and R.P.P. designed research; R.M.M., Z.C.P., and M.E.C. performed research; R.M.M., Z.C.P., J.D.R., M.E.C., S.E.P., J.R.W., and R.P.P. contributed new reagents/analytic tools; R.M.M., Z.C.P., J.D.R., M.E.C., D.B.R., and R.P.P. analyzed data; and R.M.M., Z.C.P., J.D.R., and R.P.P. wrote the paper.

## DATA AVAILABILITY STATEMENT

The data that support the findings of this study are available from the corresponding author upon reasonable request.

## ORCID

Ryan M. Mushinski  <https://orcid.org/0000-0003-3572-3500>

Jonathan D. Raff  <https://orcid.org/0000-0002-2574-8061>

Matthew E. Craig  <https://orcid.org/0000-0002-8890-7920>

Sally E. Pusede  <https://orcid.org/0000-0002-3041-0209>

Douglas B. Rusch  <https://orcid.org/0000-0002-1066-2687>

Jeffrey R. White  <https://orcid.org/0000-0002-7541-3737>

Richard P. Phillips  <https://orcid.org/0000-0002-1345-4138>

## REFERENCES

- Ambus, P., & Zechmeister-Boltenstern, S. (2007). Chapter 22 – Denitrification and N-cycling in forest ecosystems. In H. Bothe, S. J. Ferguson, & W. E. Newton (Eds.), *Biology of the nitrogen cycle* (pp. 343–358). Elsevier.
- Beidler, K. V., Phillips, R. P., Andrews, E., Fernandez, C. W., Maillard, F., Mushinski, R. M., See, C. R., & Kennedy, P. G. (2020). Substrate quality drives fungal necromass decay and decomposer community structure under contrasting vegetation types. *Journal of Ecology*, *https://doi.org/10.1111/1365-2745.13385*.
- Bouwman, A. F., Boumans, L. J. M., & Batjes, N. H. (2002). Emissions of  $N_2O$  and  $NO$  from fertilized fields: Summary of available measurement data. *Global Biogeochemical Cycles*, *16*(4), 6–1–6–13. <https://doi.org/10.1029/2001GB001811>
- Bunn, R. A., Simpson, D. T., Bullington, L. S., Lekberg, Y., & Janos, D. P. (2019). Revisiting the 'direct mineral cycling' hypothesis: Arbuscular mycorrhizal fungi colonize leaf litter, but why? *ISME Journal*, *13*(8), 1891–1898. <https://doi.org/10.1038/s41396-019-0403-2>
- Butterbach-Bahl, K., Baggs, E. M., Dannenmann, M., Kiese, R., & Zechmeister-Boltenstern, S. (2013). Nitrous oxide emissions from soils: How well do we understand the processes and their controls? *Philosophical Transactions of the Royal Society B: Biological Sciences*, *368*(1621), <https://doi.org/10.1098/rstb.2013.0122>
- Chapuis-Lardy, L., Wrage, N., Metay, A., Chotte, J. L., & Bernoux, M. (2006). Soils, a sink for  $N_2O$ ? A Review. *Global Change Biology*, *13*(1), 1–17. <https://doi.org/10.1111/j.1365-2486.2006.01280.x>
- Cheeke, T. E., Phillips, R. P., Brzostek, E. R., Rosling, A., Bever, J. D., & Fransson, P. (2017). Dominant mycorrhizal association of trees alters carbon and nutrient cycling by selecting for microbial groups with distinct enzyme function. *New Phytologist*, *214*(1), 432–442. <https://doi.org/10.1111/nph.14343>
- Cheeke, T. E., Phillips, R. P., Kuhn, A., Rosling, A. and P. Fransson. In Press. Variation in mycorrhizal hyphal production rather than turnover regulates standing fungal biomass in temperate hardwood forests. *Ecology*. <https://doi.org/10.1002/ecy.3260>.
- Cox, M. P., Peterson, D. A., & Biggs, P. J. (2010). SolexaQA: At-a-glance quality assessment of Illumina second-generation sequencing data. *BMC Bioinformatics*, *11*(1), 485. <https://doi.org/10.1186/1471-2105-11-485>
- Craig, M. E., Turner, B. L., Liang, C., Clay, K., Johnson, D. J., & Phillips, R. P. (2018). Tree mycorrhizal type predicts within-site variability in the

- storage and distribution of soil organic matter. *Global Change Biology*, 24(8), 3317–3330. <https://doi.org/10.1111/gcb.14132>
- Decock, C. (2014). Mitigating nitrous oxide emissions from corn cropping systems in the Midwestern U.S.: Potential and data gaps. *Environmental Science & Technology*, 48(8), 4247–4256. <https://doi.org/10.1021/es4055324>
- Fierer, N., & Jackson, R. B. (2006). The diversity and biogeography of soil bacterial communities. *Proceedings of the National Academy of Sciences of the United States of America*, 103(3), 626–631. <https://doi.org/10.1073/pnas.0507535103>
- Finlayson-Pitts, B. J., & Pitts Jr, J. N. (2000). Chemistry of the Upper and Lower Atmosphere. (pp. 264–293). Academic Press, Elsevier, Cambridge, Mass, USA.
- Gomez-Alvarez, V., Teal, T. K., & Schmidt, T. M. (2009). Systematic artifacts in metagenomes from complex microbial communities. *ISME Journal*, 3(11), 1314–1317. <https://doi.org/10.1038/ismej.2009.72>
- Gweon, H. S., Shaw, L. P., Swann, J., De Maio, N., AbuOun, M., Niehus, R., Hubbard, A. T. M., Bowes, M. J., Bailey, M. J., Peto, T. E. A., Hoosdally, S. J., Walker, A. S., Sebra, R. P., Crook, D. W., Anjum, M. F., Read, D. S., Stoesser, N., Abuoun, M., Anjum, M., ... on behalf of the REHAB consortium. (2019). The impact of sequencing depth on the inferred taxonomic composition and AMR gene content of metagenomic samples. *Environmental Microbiome*, 14(1), 7. <https://doi.org/10.1186/s40793-019-0347-1>
- Hansen, J., Ruedy, R., Sato, M., & Lo, K. (2010). Global surface temperature change. *Reviews of Geophysics*, 48(4). <https://doi.org/10.1029/2010RG000345>
- Herman, D. J., Firestone, M. K., Nuccio, E., & Hodge, A. (2012). Interactions between an arbuscular mycorrhizal fungus and a soil microbial community mediating litter decomposition. *FEMS Microbiology Ecology*, 80(1), 236–247. <https://doi.org/10.1111/j.1574-6941.2011.01292.x>
- Högberg, M. N., & Högberg, P. (2002). Extramatrical ectomycorrhizal mycelium contributes one-third of microbial biomass and produces, together with associated roots, half the dissolved organic carbon in a forest soil. *New Phytologist*, 154(3), 791–795. <https://doi.org/10.1046/j.1469-8137.2002.00417.x>
- Huntemann, M., Ivanova, N. N., Mavromatis, K., Tripp, H. J., Paez-Espino, D., Tennesen, K., Palaniappan, K., Szeto, E., Pillay, M., Chen, I. M., Pati, A., Nielsen, T., Markowitz, V. M., & Kyrpides, N. C. (2016). The standard operating procedure of the DOE-JGI Metagenome Annotation Pipeline (MAP vol 4). *Standards in Genomic Science*, 11, 17. <https://doi.org/10.1186/s40793-016-0138-x>
- Jain, A. K., Meiyappan, P., Song, Y., & House, J. I. (2013). CO<sub>2</sub> emissions from land-use change affected more by nitrogen cycle, than by the choice of land-cover data. *Global Change Biology*, 19(9), 2893–2906. <https://doi.org/10.1111/gcb.12207>
- Jiang, Z., McDonald, B. C., Worden, H., Worden, J. R., Miyazaki, K., Qu, Z., Henze, D. K., Jones, D. B. A., Arellano, A. F., Fischer, E. V., Zhu, L., & Boersma, K. F. (2018). Unexpected slowdown of US pollutant emission reduction in the past decade. *Proceedings of the National Academy of Sciences of the United States of America*, 115(20), 5099–5104. <https://doi.org/10.1073/pnas.1801191115>
- Jo, I., Fei, S., Oswalt, C. M., Domke, G. M., & Phillips, R. P. (2019). Shifts in dominant tree mycorrhizal associations in response to anthropogenic impacts. *Science Advances*, 5(4), eaav6358. <https://doi.org/10.1126/sciadv.aav6358>
- Kebede, M. A., Bish, D. L., Losovyj, Y., Engelhard, M. H., & Raff, J. D. (2016). The role of iron-bearing minerals in NO<sub>2</sub> to HONO conversion on soil surfaces. *Environmental Science & Technology*, 50(16), 8649–8660. <https://doi.org/10.1021/acs.est.6b01915>
- Keiluweit, M., Gee, K., Denney, A., & Fendorf, S. (2018). Anoxic microsites in upland soils dominantly controlled by clay content. *Soil Biology and Biochemistry*, 118, 42–50. <https://doi.org/10.1016/j.soilbio.2017.12.002>
- Keller, A. B., & Phillips, R. P. (2019). Leaf litter decay rates differ between mycorrhizal groups in temperate, but not tropical, forests. *New Phytologist*, 222(1), 556–564. <https://doi.org/10.1111/nph.15524>
- Kohler, A., Kuo, A., Nagy, L. G., Morin, E., Barry, K. W., Buscot, F., Canback, B., Choi, C., Cichocki, N., Clum, A., Colpaert, J., Copeland, A., Costa, M. D., Dore, J., Floudas, D., Gay, G., Girlanda, M., Henrissat, B., Herrmann, S., ... Martin, F. (2015). Convergent losses of decay mechanisms and rapid turnover of symbiosis genes in mycorrhizal mutualists. *Nature Genetics*, 47(4), 410–415. <https://doi.org/10.1038/ng.3223>
- Kuzyakov, Y. (2010). Priming effects: Interactions between living and dead organic matter. *Soil Biology and Biochemistry*, 42(9), 1363–1371. <https://doi.org/10.1016/j.soilbio.2010.04.003>
- Kuzyakov, Y., & Blagodatskaya, E. (2015). Microbial hotspots and hot moments in soil: Concept & review. *Soil Biology and Biochemistry*, 83, 184–199. <https://doi.org/10.1016/j.soilbio.2015.01.025>
- Langmead, B., Trapnell, C., Pop, M., & Salzberg, S. L. (2009). Ultrafast and memory-efficient alignment of short DNA sequences to the human genome. *Genome Biology*, 10(3), R25. <https://doi.org/10.1186/gb-2009-10-3-r25>
- Levy-Booth, D. J., Prescott, C. E., & Grayston, S. J. (2014). Microbial functional genes involved in nitrogen fixation, nitrification and denitrification in forest ecosystems. *Soil Biology and Biochemistry*, 75, 11–25. <https://doi.org/10.1016/j.soilbio.2014.03.021>
- Li, H. (2015). BFC: Correcting Illumina sequencing errors. *Bioinformatics*, 31(17), 2885–2887. <https://doi.org/10.1093/bioinformatics/btv290>
- Lin, G., McCormack, M. L., Ma, C., & Guo, D. (2017). Similar below-ground carbon cycling dynamics but contrasting modes of nitrogen cycling between arbuscular mycorrhizal and ectomycorrhizal forests. *New Phytologist*, 213(3), 1440–1451. <https://doi.org/10.1111/nph.14206>
- Lindahl, B. D., & Tunlid, A. (2015). Ectomycorrhizal fungi – Potential organic matter decomposers, yet not saprotrophs. *New Phytologist*, 205(4), 1443–1447. <https://doi.org/10.1111/nph.13201>
- Lladó, S., López-Mondéjar, R., & Baldrian, P. (2017). Forest soil bacteria: Diversity, involvement in ecosystem processes, and response to global change. *Microbiology and Molecular Biology Reviews*, 81(2), e00063–e16. <https://doi.org/10.1128/MMBR.00063-16>
- Lu, C., & Tian, H. (2017). Global nitrogen and phosphorus fertilizer use for agriculture production in the past half century: Shifted hot spots and nutrient imbalance. *Earth System Science Data*, 9(1), 181–192. <https://doi.org/10.5194/essd-9-181-2017>
- Maharjan, B., & Venterea, R. T. (2014). Anhydrous ammonia injection depth does not affect nitrous oxide emissions in a silt loam over two growing seasons. *Journal of Environmental Quality*, 43(5), 1527–1535. <https://doi.org/10.2134/jeq2014.07.0292>
- Midgley, M. G., Brzostek, E., Phillips, R. P., & Austin, A. (2015). Decay rates of leaf litters from arbuscular mycorrhizal trees are more sensitive to soil effects than litters from ectomycorrhizal trees. *Journal of Ecology*, 103(6), 1454–1463. <https://doi.org/10.1111/1365-2745.12467>
- Midgley, M. G., & Phillips, R. P. (2014). Mycorrhizal associations of dominant trees influence nitrate leaching responses to N deposition. *Biogeochemistry*, 117(2–3), 241–253. <https://doi.org/10.1007/s10553-013-9931-4>
- Midgley, M. G., & Phillips, R. P. (2016). Resource stoichiometry and the biogeochemical consequences of nitrogen deposition in a mixed deciduous forest. *Ecology*, 97(12), 3369–3378. <https://doi.org/10.1002/ecy.1595>
- Mushinski, R. M., Phillips, R. P., Payne, Z. C., Abney, R. B., Jo, I., Fei, S., Pusede, S. E., White, J. R., Rusch, D. B., & Raff, J. D. (2019). Microbial mechanisms and ecosystem flux estimation for aerobic NO<sub>y</sub> emissions from deciduous forest soils. *Proceedings of the National Academy of Sciences of the United States of America*, 116(6), 2138–2145. <https://doi.org/10.1073/pnas.1814632116>

- Nurk, S., Meleshko, D., Korobeynikov, A., & Pevzner, P. A. (2017). metaSPAdes: A new versatile metagenomic assembler. *Genome Research*, 27(5), 824–834. <https://doi.org/10.1101/gr.213959.116>
- Paterson, E., Sim, A., Davidson, J., & Daniell, T. J. (2016). Arbuscular mycorrhizal hyphae promote priming of native soil organic matter mineralisation. *Plant and Soil*, 408(1–2), 243–254. <https://doi.org/10.1007/s11104-016-2928-8>
- Persson, T., Rudebeck, A., Jussy, J. H., Colin-Belgrand, M., Priemé, A., Dambrine, E., Karlsson, P. S., & Sjöberg, R. M. (2000). Soil nitrogen turnover – Mineralisation, nitrification and denitrification in European forest soils. In E.-D. Schulze (Ed.), *Carbon and nitrogen cycling in European forest ecosystems* (pp. 297–311). Springer. [https://doi.org/10.1007/978-3-642-57219-7\\_14](https://doi.org/10.1007/978-3-642-57219-7_14)
- Phillips, R. P., Brzostek, E., & Midgley, M. G. (2013). The mycorrhizal-associated nutrient economy: A new framework for predicting carbon–nutrient couplings in temperate forests. *New Phytologist*, 199(1), 41–51. <https://doi.org/10.1111/nph.12221>
- Pilegaard, K. (2013). Processes regulating nitric oxide emissions from soils. *Philosophical Transactions of the Royal Society B: Biological Sciences*, 368(1621), <https://doi.org/10.1098/rstb.2013.0126>
- Read, D. J. (1991). Mycorrhizas in ecosystems. *Experientia*, 47(4), 376–391. <https://doi.org/10.1007/bf01972080>
- Reed, C., Brumby, C. A., Crilley, L. R., Kramer, L. J., Bloss, W. J., Seakins, P. W., Lee, J. D., & Carpenter, L. J. (2016). HONO measurement by differential photolysis. *Atmospheric Measurement Techniques*, 9, 2483–2495. <https://doi.org/10.5194/amt-9-2483-2016>
- Robertson, G. P., & Tiedje, J. M. (1987). Nitrous oxide sources in aerobic soils: Nitrification, denitrification and other biological processes. *Soil Biology and Biochemistry*, 19(2), 187–193. [https://doi.org/10.1016/0038-0717\(87\)90080-0](https://doi.org/10.1016/0038-0717(87)90080-0)
- Romer, P. S., Duffey, K. C., Wooldridge, P. J., Edgerton, E., Baumann, K., Feiner, P. A., Miller, D. O., Brune, W. H., Koss, A. R., de Gouw, J. A., Misztal, P. K., Goldstein, A. H., & Cohen, R. C. (2018). Effects of temperature-dependent NO<sub>x</sub> emissions on continental ozone production. *Atmospheric Chemistry and Physics*, 18(4), 2601–2614. <https://doi.org/10.5194/acp-18-2601-2018>
- Ruan, L., Bhardwaj, A. K., Hamilton, S. K., & Robertson, G. P. (2016). Nitrogen fertilization challenges the climate benefit of cellulosic biofuels. *Environmental Research Letters*, 11(6), <https://doi.org/10.1088/1748-9326/11/6/064007>
- Scharko, N. K., Schütte, U. M. E., Berke, A. E., Banina, L., Peel, H. R., Donaldson, M. A., Hemmerich, C., White, J. R., & Raff, J. D. (2015). Combined flux chamber and genomics approach links nitrous acid emissions to ammonia oxidizing bacteria and Archaea in urban and agricultural soil. *Environmental Science & Technology*, 49(23), 13825–13834. <https://doi.org/10.1021/acs.est.5b00838>
- Schwede, D. B., Simpson, D., Tan, J., Fu, J. S., Dentener, F., Du, E., & deVries, W. (2018). Spatial variation of modelled total, dry and wet nitrogen deposition to forests at global scale. *Environmental Pollution*, 243(Pt B), 1287–1301. <https://doi.org/10.1016/j.envpol.2018.09.084>
- Schwertmann, U. (1973). Use of oxalate for Fe extraction from soils. *Canadian Journal of Soil Science*, 53(2), 244–246. <https://doi.org/10.4141/cjss73-037>
- Scott, N. A., & Binkley, D. (1997). Foliage litter quality and annual net N mineralization: Comparison across North American forest sites. *Oecologia*, 111(2), 151–159. <https://doi.org/10.1007/s004420050219>
- Simon, H., Reff, A., Wells, B., Xing, J., & Frank, N. (2015). Ozone trends across the United States over a period of decreasing NO<sub>x</sub> and VOC emissions. *Environmental Science & Technology*, 49(1), 186–195. <https://doi.org/10.1021/es504514z>
- Soares, J. R., Cassman, N. A., Kielak, A. M., Pijl, A., Carmo, J. B., Lourenco, K. S., Laanbroek, H. J., Cantarella, H., & Kuramae, E. E. (2016). Nitrous oxide emission related to ammonia-oxidizing bacteria and mitigation options from N fertilization in a tropical soil. *Scientific Reports*, 6, 30349. <https://doi.org/10.1038/srep30349>
- Steidinger, B. S., Crowther, T. W., Liang, J., Van Nuland, M. E., Werner, G. D. A., Reich, P. B., Nabuurs, G. J., de-Miguel, S., Zhou, M., Picard, N., Herault, B., Zhao, X., Zhang, C., Routh, D., & Peay, K. G. (2019). Climatic controls of decomposition drive the global biogeography of forest-tree symbioses. *Nature*, 569(7756), 404–408. <https://doi.org/10.1038/s41586-019-1128-0>
- Steinkamp, J., Ganzeveld, L. N., Wilcke, W., & Lawrence, M. G. (2009). Influence of modelled soil biogenic NO emissions on related trace gases and the atmospheric oxidizing efficiency. *Atmospheric Chemistry & Physics*, 9(8), 2663–2677. <https://doi.org/10.5194/acp-9-2663-2009>
- Subbarao, G. V., Sahrawat, K. L., Nakahara, K., Rao, I. M., Ishitani, M., Hash, C. T., Kishii, M., Bonnett, D. G., Berry, W. L., & Lata, J. C. (2013). A paradigm shift towards low-nitrifying production systems: The role of biological nitrification inhibition (BNI). *Annals of Botany*, 112(2), 297–316. <https://doi.org/10.1093/aob/mcs230>
- Talbot, J. M., Allison, S. D., & Treseder, K. K. (2008). Decomposers in disguise: Mycorrhizal fungi as regulators of soil C dynamics in ecosystems under global change. *Functional Ecology*, 22(6), 955–963. <https://doi.org/10.1111/j.1365-2435.2008.01402.x>
- Ullah, S., & Moore, T. R. (2011). Biogeochemical controls on methane, nitrous oxide, and carbon dioxide fluxes from deciduous forest soils in eastern Canada. *Journal of Geophysical Research*, 116(G3), <https://doi.org/10.1029/2010Jg001525>
- Ulmer, M. G., Knuteson, J. A., & Patterson, D. D. (1994). Particle size analysis by hydrometer: A routine method for determining clay fraction. *Soil Survey Horizons*, 35(1), 11–17. <https://doi.org/10.2136/sh1994.1.0011>
- van Dijk, S. M., Gut, A., Kirkman, G. A., Gomes, B. M., Meixner, F. X., & Andreae, M. O. (2002). Biogenic NO emissions from forest and pasture soils: Relating laboratory studies to field measurements. *Journal of Geophysical Research: Atmospheres*, 107(D20), LBA 25-1–LBA 25-11. <https://doi.org/10.1029/2001JD000358>
- Wang, H., Marshall, C. W., Cheng, M., Xu, H., Li, H., Yang, X., & Zheng, T. (2017). Changes in land use driven by urbanization impact nitrogen cycling and the microbial community composition in soils. *Scientific Reports*, 7, 44049. <https://doi.org/10.1038/srep44049>
- Wright, S. F., Starr, J. L., & Paltineanu, I. C. (1999). Changes in aggregate stability and concentration of Glomalin during tillage management transition. *Soil Science Society of America Journal*, 63(6), 1825–1829. <https://doi.org/10.2136/sssaj1999.6361825x>
- Zhu, K., McCormack, M. L., Lankau Richard, A., Egan, J. F., & Wurzburger, N. (2018). Association of ectomycorrhizal trees with high carbon-to-nitrogen ratio soils across temperate forests is driven by smaller nitrogen not larger carbon stocks. *Journal of Ecology*, 106(2), 524–535. <https://doi.org/10.1111/1365-2745.12918>

## SUPPORTING INFORMATION

Additional supporting information may be found online in the Supporting Information section.

**How to cite this article:** Mushinski RM, Payne ZC, Raff JD, et al. Nitrogen cycling microbiomes are structured by plant mycorrhizal associations with consequences for nitrogen oxide fluxes in forests. *Glob Change Biol*. 2021;27:1068–1082. <https://doi.org/10.1111/gcb.15439>